

Confinement of CdS Nanocrystals in a Sonogel Matrix

R. LITRÁN

*Departamento de Física de la Materia Condensada, Universidad de Cádiz, Apdo, 40,
Puerto Real (11510) Cádiz, Spain*

R. ALCÁNTARA

Departamento de Química-Física, Universidad de Cádiz, Apdo, 40, Puerto Real (11510) Cádiz, Spain

E. BLANCO AND M. RAMÍREZ-DEL-SOLAR

*Departamento de Física de la Materia Condensada, Universidad de Cádiz, Apdo, 40,
Puerto Real (11510) Cádiz, Spain*

Abstract. CdS/silica xerogel composites have been prepared using a sonocatalytic method. The confinement effects of CdS semiconductor nanocrystallites have been analyzed through UV-VIS absorption and Raman scattering. The blue shift of the absorption band and the shape of the Low Frequency Inelastic Raman Scattering (LOFIRS) spectra make it possible to evaluate the size of nanocrystallites, which are contrasted with previous results obtained through other techniques. Moreover, in the 200–700 cm^{-1} region of Raman shift, resonant effects are discussed, through the longitudinal optical mode lines.

Keywords: sonogel, nanocomposite, quantum dot, Raman scattering, LOFIRS, UV-VIS absorption, CdS

1. Introduction

The future evolution of integrated nonlinear optics depends on the performances that nonlinear optical materials can achieve. Nevertheless, nature has not been generous to the optical nonlinearities of bulk optical materials; in the case of integrated nonlinear optics, the situation is aggravated by additional requirements on the materials as regards their processability, adaptability and interfacing with other materials [1–3].

One way to enhance the cubic nonlinearities of materials with very delocalized electrons, such as semiconductors, is to artificially confine the valence electrons in regions much shorter than their natural delocalization length in the bulk, which extends over many unit cells. These materials are characterized by broad but discrete optical resonances whose position, oscillator strength and dynamics depend on the extension of the artificial confinement and hence can be modified to meet certain requirements.

The sol-gel process allows the production of silica matrices with a higher semiconductor concentration at temperatures significantly lower than those required by the classic melting methods [4–6]. Furthermore, sonocatalysis is a good approach for the improvement of the nonlinear properties of the composites, as regards the narrower size distribution of the nanocrystals induced in matrices presenting a finer porosity. In this sense, our previous papers proved that this method yields CdS-sonogel composites whose particle size distribution and absorption behaviour are consistent with the Efros and Efros model for intermediate degrees of quantum confinement [7]. However, as we will describe in the present paper, the ageing behaviour of these samples reveals a low stability of the nanocrystals formed in these conditions. An optimization of the composite processing is therefore required in order to increase the composite performance. For this purpose, diverse experimental parameters were tested and their influence on the sample characteristics evaluated.

2. Experimental

Optically transparent silica sono-xerogel monoliths were prepared by ultrasound-promoted hydrolysis of TMOS : water : formamide mixtures, doped with different cadmium doses, as described in [7]. Once the solutions gelled at room temperature, they were left to age for one week in a closed container and then dried for at least two weeks in a partially dry atmosphere.

Diverse experimental parameters have been varied from piece to piece in order to optimize the sample composition and preparation conditions. Hence, pH = 2 and strongly acid [8] hydrolysis water, and cadmium doping doses leading to a final 1, 3, 5 or 10 CdS wt.% (if complete conversion) were used for composite processing.

Cadmium-doped samples were heat-treated in air, at temperatures in 200–500°C range. After cooled at room temperature, the CdO-composites were exposed to H₂S gas at 150°C, in order to precipitate CdS nanocrystals. After 1 hour exposure, temperature was further increased up to 500 and 800°C in a N₂-flow atmosphere.

Raman measurements were obtained with the 514.5 nm line of an Argon-ion (Ar⁺) laser Spectra-Physics (model 168). The scattered light was collected at 90° as to the incident laser beam and was analyzed with a double monochromator, Jobin-Yvon model U 1000. A cooled photomultiplier (model RCA 31034), and a photon counting system were used to collect the signal which was processed by a PC. All the spectra were obtained at room temperature with approximately 300 mW laser power on the sample. The slit widths used led to a spectral resolution of ± 2.5 cm⁻¹. The laser beam was focused inside the sample, which was the analyzed zone.

Various alternative excitation laser lines such as 488.0, 476.5 and 457.9 nm have been tested. However, the best results have been obtained with the 514.5 nm laser line for all composites.

Linear UV-VIS Absorption of the samples was measured at room temperature in the 300–900 nm range using a VARIAN Cary 31 spectrophotometer. For a better comparison of the various samples, the absorption band is in some cases discussed with regard to derivative curves. The peak position gives us the semiconductor gap energy from which an average nanocrystal size can be evaluated by means of Efros and Efros expression [9].

The sample behaviour during heating from room temperature up to 800°C was characterized from the thermograms registered in a Perkin-Elmer TGA-7.

3. Results and Discussion

Samples prepared at room temperature using sono-catalysis present, as described before [7], a very promising absorption behaviour. Nevertheless, these samples exhibit an ageing effect, presumably because of the low stability of the nanocrystals in the silica matrix, leading to a gradual nanocomposite degradation. A typical example of this effect is presented in Fig. 1, where the absorption spectra registered for a 5% CdS composite are compared at different moments three weeks apart. A remarkable decrease in the absorption band intensity of the recently diffused xerogel is observed during ageing, but there is no important peak position shift. In order to improve this very low time stability, avoiding the nanocrystals re-dissolution in the xerogel liquid phase, xerogels were heated in air before H₂S diffusion.

Figure 2 shows Raman scattering results for liquid formamide and 1% composite treated at different temperatures. The 1LO (longitudinal optical) phonon frequency for a single CdS crystal was given in the literature [10] as 305 cm⁻¹, and the corresponding overtone (2LO) at 610 cm⁻¹ [11]. At room temperature (plot b), these modes are not observed, probably because the number and size of particles are not enough to appreciate the CdS modes. In fact, plot b shows a band at 602 cm⁻¹ indicating the formamide contribution to the Raman signal (plot a) and a second one at 490 cm⁻¹ assigned to silica structural modes [12]. In order to obtain formamide-free composites, they must be preheated over 270°C [13] for removing organics from xerogel structures. However, this change will transform CdS particle generation, from mainly a precipitation process, Cd²⁺ + H₂S(g) → CdS(s), to a complete cadmium oxide sulphuration, CdO(s) + H₂S(g) → CdS(s). In this way, a more complete CdO particle generation is produced when xerogels are heated over 400°C. Diverse experiments revealed that in order to obtain carbon-free samples, oxidation treatments should go up to 500°C [14].

When xerogels are submitted to increasing temperatures, monolithicity of the final material is strongly dependent on the textural properties of the starting material. In this sense, diverse parameters have

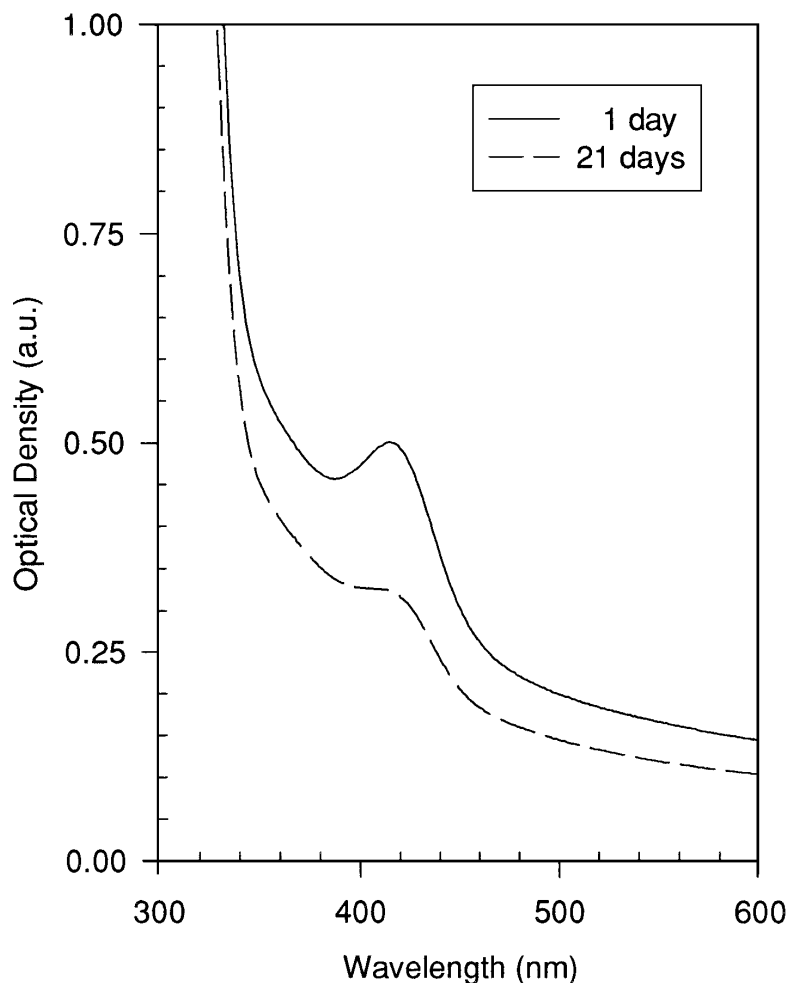


Figure 1. Evolution with ageing of UV-VIS absorption spectra of a CdS composite. Degradation of the sample is pointed out by the intensity decrease of the CdS absorption band.

been considered. It is well known that both lower pH and the use of ultrasound lead to xerogels with finer porosity, whereas the opposite is induced by the formamide content which, on the other hand, keeps xerogels from cracking. In previous works [7, 15] we proved that better composite processing parameters for smaller and narrower porosity were $Rw = 10$, $R_f = 3$, $\text{pH} < 1$ and an ultrasound energy of $60 \text{ J}\cdot\text{cm}^{-3}$, when composites were obtained at room temperature. Furthermore, we concluded that increasing sonosol cadmium salt content leads to narrower pore size distributions with a slight increase in the mean pore radius.

For the present work, it was however necessary to change these experimental conditions in order to avoid

samples cracking when heated over 200°C . Regarding the pH of the hydrolysis water, despite the finer porosity of the samples prepared at $\text{pH} < 1$ [8], it was found that only an increase in the sonosol pH allows the xerogel to be heated over 500°C without cracking. DTG in Fig. 3 illustrates the different behaviour of samples prepared at $\text{pH} < 1$ and $\text{pH} = 2$ when heated.

In view of the more open porosity of the $\text{pH} = 2$ sample, the elimination of chemicals from the porous structure takes place at a lower temperature than it does for the $\text{pH} < 1$ sample, for which two steps can be distinguished. This explains the higher monolithic sample yield after oxidation in the first case. Consequently, we will now focus on samples prepared with that condition, $\text{pH} = 2$.

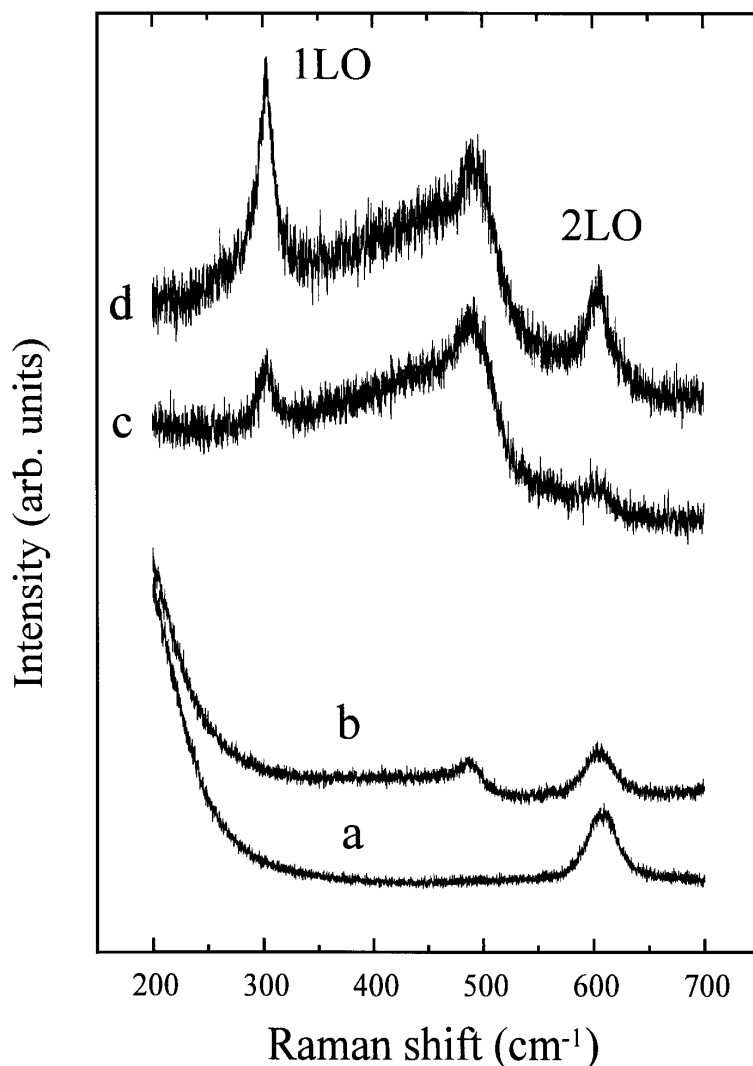


Figure 2. Raman spectra for 1% CdS composite after heat-treatment at (b) 100°C, (c) 500°C and (d) 800°C. For comparison, spectra obtained for liquid formamide is included as curve (a).

The thermal evolution of the 1% CdS composite can be analysed from the Raman spectra in Fig. 2, where the CdS longitudinal optical modes can be observed for pre-heated samples (c and d spectra). However, the 1LO band appears at 301 cm^{-1} and its corresponding overtone, 2LO, at 602 cm^{-1} . These band shifts to lower frequencies as to the bulk CdS are due to the effect of particle size [10, 16–19] on the vibrational properties in small crystallites. When the composite is treated at 800°C in N_2 flow, the Raman peaks present higher intensity, due to an increase in the composite particle density during sintering [20].

Figure 4 shows the Raman spectra recorded for a series of samples heated at 500°C, with different cadmium loads. All curves show the 490 cm^{-1} band corresponding to the silica network and the LO modes. The signal intensity increases along with CdS concentration, even if no noticeable changes of the band position are observed.

The size distribution of CdS nanocrystals can be determined using the *low frequency inelastic Raman scattering* (LOFIRS), previously used by several authors [11, 21]. The interaction of the laser light with the normal modes of a nanocrystal gives rise to a

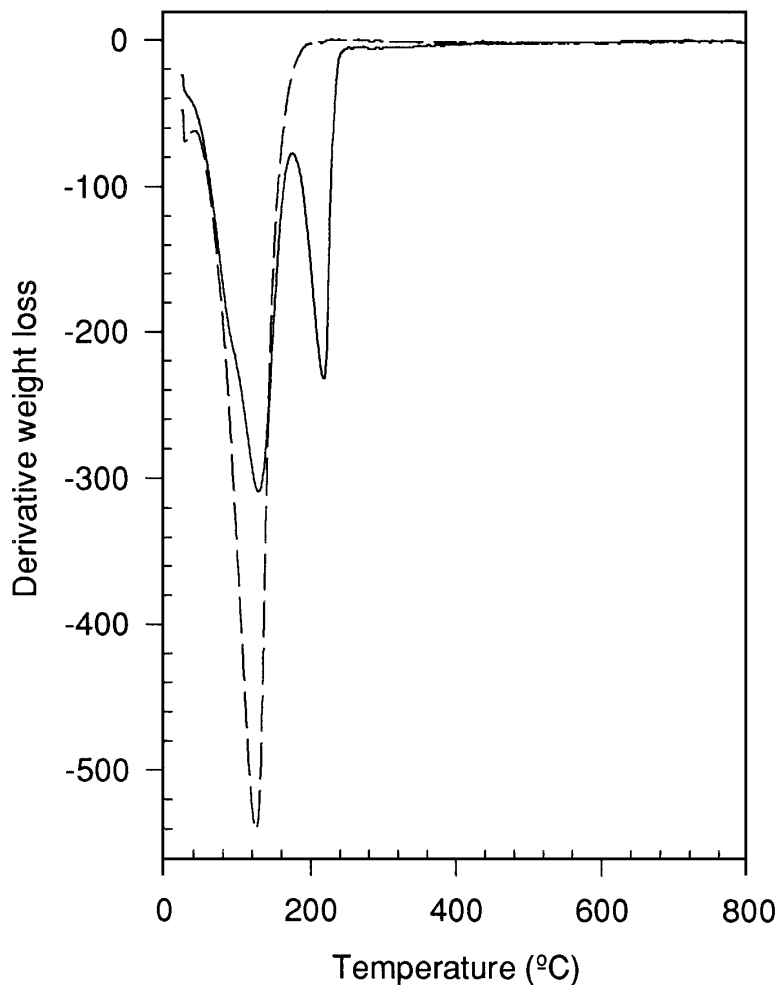


Figure 3. DTG registered for xerogels prepared at pH < 1 (—) and pH = 2 (---).

low-frequency inelastic scattering line close to the Rayleigh line, LOFIRS [21, 22]. Small crystalline particles in a glassy matrix can be considered in a first approximation as an elastic body and vibrate according to different eigenmodes, the frequency of these modes being a function of their diameter d . Through high resolution electron microscopy, we have observed that the approximation of a spherical shape for the CdS particles is valid [23]. The breathing mode, which is observed, does not depolarize the laser light. The diameter of the particles is deduced from the measured low frequency ω_0 peak using the relation [21]:

$$d = \frac{0.9\nu_1}{\omega_0 c} \quad (1)$$

ν_1 is the bulk CdS longitudinal sound speed (4200 ms^{-1}) and c is the light speed.

Figure 5 shows low frequency Raman spectra, once corrected from silica background, for 1% CdS samples heated at 500 and 800°C in N_2 atmosphere. Notice the band position shift when the CdS composite is heated from 500 to 800°C. According to Eq. (1), this behaviour indicates a semiconductor nanoparticle growth at increasing temperatures. When this heat-treatment is performed in air, oxidation process is significant and colorless samples result.

Figure 6 shows the UV-VIS absorption results, for the corresponding samples in Fig. 4, as the optical density derivative, which allows a more precise determination of the absorption band position. The increase

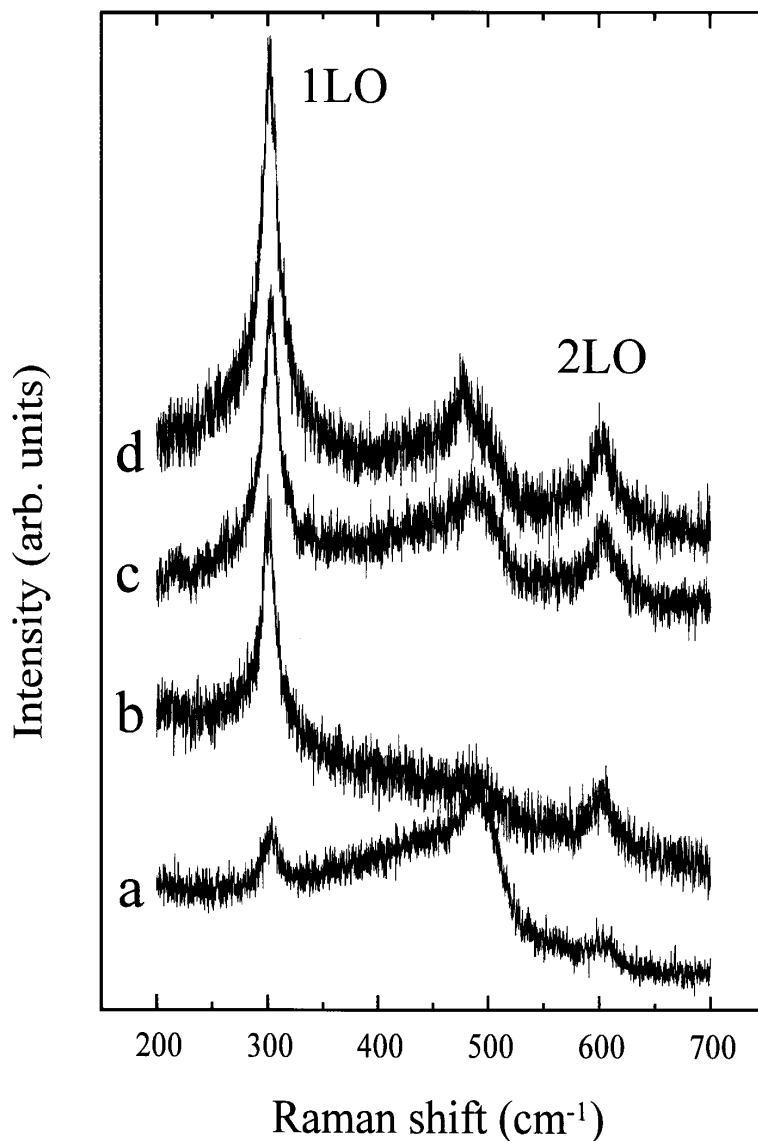


Figure 4. Raman scattering showing longitudinal optical modes: (a), (b), (c) and (d) correspond to 1, 3, 5 and 10 wt.% CdS concentration respectively. All the samples are treated at 500°C.

in CdS content involves two main features: a band red-shift, which can be related to larger semiconductor crystallites according to the Efros model, and wider derivative peaks, probably due to a spreading of the particle size. This agrees with the observed increase in the Raman band intensity as the amount of CdS becomes larger (Fig. 4). Experimentally, we found that the absorption intensity remains constant with time for all these samples in contrast with the non-treated samples

as shown in Fig. 1. In addition, the mechanical behaviour of the composites is also improved and water absorption is no noticeable.

Table 1 presents the semiconductor particle size calculated through both methods. Sizes obtained from absorption curves are systematically lower than those calculated from LOFIRS band positions, but both series follow the same trend, increasing with cadmium content and temperature. It should be mentioned that

Table 1. Diameter of CdS nanocrystallites calculated by Raman LOFIRS and absorption (Efros and Efros model).

| % CdS | Temperature (°C) | d Raman (nm) | d Absorption (nm) |
|-------|------------------|----------------|---------------------|
| 1 | 800 | 5.0 | 4.5 |
| 1 | 500 | 4.5 | 4.0 |
| 3 | 500 | 6.5 | 6.0 |
| 5 | 500 | 5.5 | — |
| 10 | 500 | 5.5 | — |

the Efros and Efros Model is no longer applicable for a Cd content higher than 5%, because the band position does not show any evidence of the quantum confinement effect. However, particle sizes evaluated from these samples through Raman scattering are lower than those obtained for 3%, which could be due to the presence of nanocrystal aggregates because of the larger oversaturation values involved. These results present a good agreement with those obtained from previous experiments (TEM, Small Angle Scattering) [7, 24].

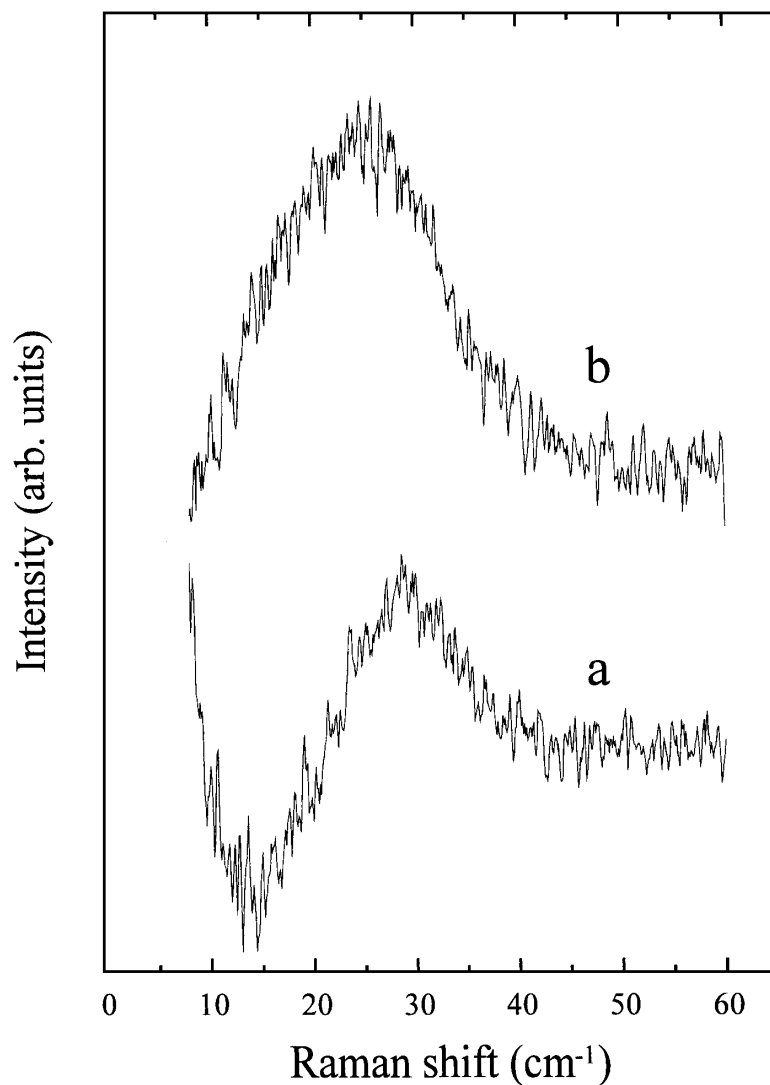


Figure 5. Raman scattering showing low frequency modes for 1% CdS: (a) heated at 500°C and (b) at 800°C.

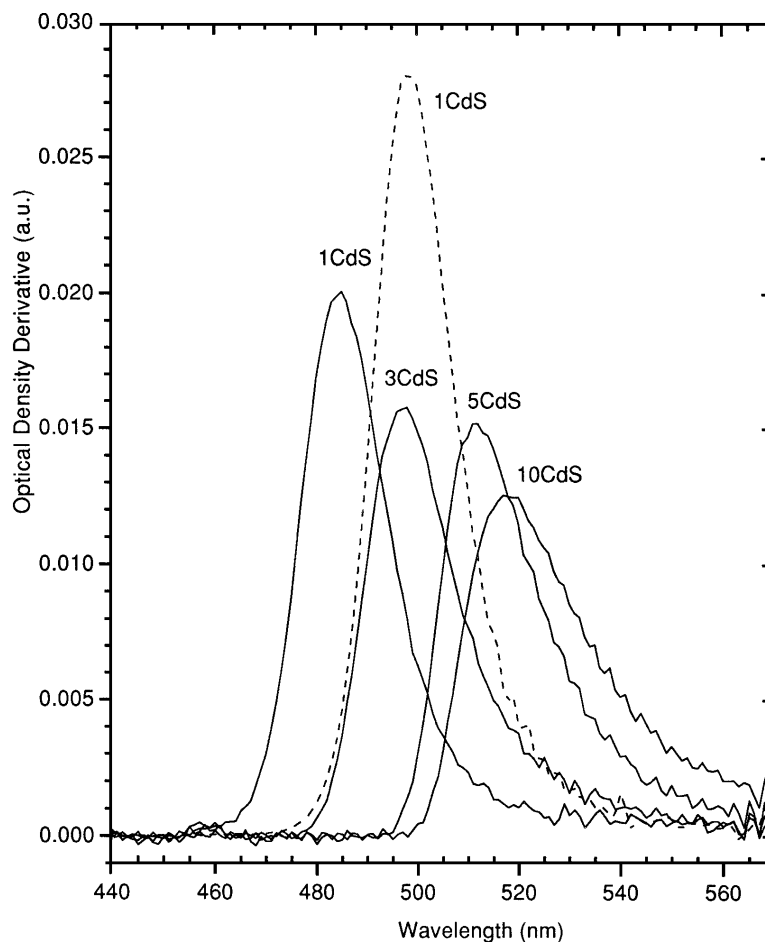


Figure 6. Comparison of the UV-VIS absorption behavior of CdS-composites heat-treated at 500°C (—) and 800°C (---) with different nominal composition: (a) 1% CdS, (b) 3% CdS, (c) 5% CdS and (d) 10% CdS.

4. Conclusions

A thermal treatment has been designed which makes it possible to obtain stable composites showing quantum confinement without ageing effect. LOFIRS results lead to nanocrystalite sizes of 4–6 nm, which are in agreement with those obtained from the Efros and Efros Model. At high CdS concentration, the aggregation of semiconductor particles is responsible for the quantum confinement effect no longer being observed. Hence, in order to increase the CdS load in the composites, a previous chemical stabilization process is necessary.

Acknowledgments

This work is supported by the Consejería de Educación de la Junta de Andalucía (exp.#6015) and by the

Ministerio de Educación y Ciencia (PFPI and CICYT proj.#MAT-95-0040-C02-02).

References

1. C. Flytzanis, *Nonlinear Optics; Materials and Devices*, edited by C. Flytzanis and J.L. Oudar (Springer Verlag, Berlin, 1986).
2. C. Flytzanis, *Nonlinear Optics Materials Principles and Applications*, edited by V. Digiorgio and C. Flytzanis (North Holland Co., Amsterdam, 1994).
3. C. Flytzanis, *Nonlinear Optical Material for Integrated Optics: First Summer School on Nonlinear Optics* (U.A.M., Madrid, 1994).
4. M. Nogami, S. Suzuki, and K. Nagasaka, *J. of Non-Crystalline Solids* **135**, 182 (1991).
5. M. Yamane, T. Takada, J.D. Mackenzie, and C.Y. Li, *SPIE Sol-Gel Optics II* **1758**, 577 (1992).
6. L. Spanhel, E. Arpac, and H. Schmidt, *J. of Non-Crystalline Solids* **147&148**, 657 (1992).

7. M. Piñero, R. Litrán, C. Fernández-Lorenzo, E. Blanco, M. Ramírez-del-Solar, N. de la Rosa-Fox, L. Esquivias, A. Craievich, and J. Zarzycki, *J. of Sol-Gel Science and Technology* **2**, 689 (1994).
8. L.L. Hench, *Science of Ceramic Chemical Processing*, edited by L.L. Hench and D.R. Ulrich (Wiley, NY, 1986), p. 52.
9. Al. L. Éfros and A. Éfros, *Sov. Phys. Semicond.* **16**(7), 772 (1982).
10. R.J. Briggs and A.K. Ramdas, *Phys. Rev. B* **13**, 5518 (1976).
11. M. Ferrari, B. Champagnon, and M. Barland, *J. Non-Cryst. Solids* **151**, 95 (1992).
12. C.J. Brinker and G.W. Scherer, *Sol-Gel Science: The Physics and Chemistry of Sol-Gel Processing* (Academic Press Inc., San Diego, 1990), p. 543.
13. E. Blanco, M. Ramírez-del-Solar, N. de la Rosa-Fox, and L. Esquivias, *Materials Letters* **22**, 265 (1995).
14. T. Takada, C. Li, J.Y. Tseng, and J.D. Mackenzie, *J. of Sol-Gel Science and Technology* **1**, 123 (1994).
15. E. Blanco, R. Litrán, M. Ramírez-del-Solar, N. de la Rosa-Fox, and L. Esquivias, *J. Mat. Res.* **9**, 2873 (1994).
16. J.F. Scott and T.C. Damen, *Opt. Commun.* **5**, 410 (1972).
17. R. Rosetti, S. Nakahara, and L.E. Brus, *J. Chem. Phys.* **82**, 552 (1985).
18. H. Jerominek, M. Pigeon, S. Patela, Z. Jakubczk, C. Delisle, and R. Tremblay, *J. Appl. Phys.* **63**, 957 (1988).
19. C.M. Dai, L. Horng, W.F. Hsieh, Y.T. Shih, C.T. Tsai, and D.S. Chuu, *J. Vac. Sci. Technol. A* **10**, 484 (1992).
20. N. de la Rosa-Fox, E. Blanco, and L. Esquivias, VIIIth Int. Conf. on the Physics of Non-Crystalline Solids, 29 June–1 July, 1995 (Turku, Finland) (accepted for pub. in *J. Non-Cryst. Solids*).
21. B. Champagnon, B. Andrianasolo, and E. Duval, *J. Chem. Phys.* **94**, 5237 (1991).
22. E. Duval, A. Boukenter, and B. Champagnon. *Phys. Rev. Lett.* **56**, 2052 (1986).
23. A. Othmani, C. Bovier, J.C. Plenet, J. Dumas, B. Champagnon, and C. Mai, *Mat. Sci. & Eng. A* **168**, 263 (1993).
24. A. Craievich, N. de la Rosa-Fox, E. Blanco, M. Piñero, M. Ramírez-del-Solar, and L. Esquivias, *NanoStructured Materials* **5**(3), 363 (1995).